

Geological Society of America Bulletin

A biocalcification crisis at the Triassic-Jurassic boundary recorded in the Budva Basin (Dinarides, Montenegro)

Alenka E. Crne, Helmut Weissert, Spela Gorican and Stefano M. Bernasconi

Geological Society of America Bulletin 2011;123;40-50
doi: 10.1130/B30157.1

Email alerting services

click www.gsapubs.org/cgi/alerts to receive free e-mail alerts when new articles cite this article

Subscribe

click www.gsapubs.org/subscriptions/ to subscribe to Geological Society of America Bulletin

Permission request

click <http://www.geosociety.org/pubs/copyrt.htm#gsa> to contact GSA

Copyright not claimed on content prepared wholly by U.S. government employees within scope of their employment. Individual scientists are hereby granted permission, without fees or further requests to GSA, to use a single figure, a single table, and/or a brief paragraph of text in subsequent works and to make unlimited copies of items in GSA's journals for noncommercial use in classrooms to further education and science. This file may not be posted to any Web site, but authors may post the abstracts only of their articles on their own or their organization's Web site providing the posting includes a reference to the article's full citation. GSA provides this and other forums for the presentation of diverse opinions and positions by scientists worldwide, regardless of their race, citizenship, gender, religion, or political viewpoint. Opinions presented in this publication do not reflect official positions of the Society.

Notes

A biocalcification crisis at the Triassic-Jurassic boundary recorded in the Budva Basin (Dinarides, Montenegro)

Alenka E. Črne^{1,†}, Helmut Weissert², Špela Goričan¹, and Stefano M. Bernasconi²

¹*Ivan Rakovec Institute of Palaeontology, ZRC SAZU, Novi trg 2, SI-1000 Ljubljana, Slovenia*

²*Geological Institute, Universitätstrasse 16, ETH-Zürich, CH-8092 Zürich, Switzerland*

ABSTRACT

Volcanic activity in the Central Atlantic magmatic province, resulting in an increased flux of CO₂, SO₂, and CH₄ into the oceans and atmosphere, has been proposed as one of the mechanisms causing the biotic crisis at the Triassic-Jurassic boundary. Oceanic uptake of CO₂ due to extreme greenhouse conditions should have had an impact on ocean chemistry and the position of the calcite compensation depth. In this study, we chose two pelagic sections from the Budva Basin as archives for paleoceanographic change across the Triassic-Jurassic boundary in deep-water settings. Our record represents the first documentation of a sudden termination of carbonate deposition across the Triassic-Jurassic boundary in a pelagic deep-water environment. Based on radiolarian biostratigraphy, the system boundary is placed at the sharp lithological contact between two pelagic formations, the Upper Triassic limestones and Lower Jurassic siliceous limestones alternating with shales. A rapid drop of carbonate content from 90% to less than 10% occurred contemporaneous with a negative anomaly in the stable carbon isotope record measured in both bulk carbonate (1.3‰) and bulk organic matter (1.1‰). The abrupt reduction of carbonate content in the Budva Basin was the result of either increased carbonate dissolution causing shoaling of the calcite compensation depth or reduced carbonate input due to biocalcification crisis. Both nonexclusive scenarios support the hypothesis of decreased ocean saturation with respect to calcium carbonate, which could be a direct consequence of increased CO₂, SO₂, and CH₄ fluxes.

INTRODUCTION

The mass extinction at the Triassic-Jurassic (T-J) boundary is considered to be among the five largest events of the Phanerozoic (Sepkoski,

1996; ranked as the third largest ecological crisis by McGhee et al., 2004; for alternative view, see Bambach, 2006). The processes proposed to explain the end-Triassic mass extinction range from gradualistic (e.g., Tanner et al., 2004) to catastrophic. The latter is supported by rapid biotic turnovers across the boundary among marine biota, e.g., ammonoids, radiolarians, brachiopods (Guex et al., 2004; Carter and Hori, 2005; Tomašových and Siblík, 2007), and also among terrestrial vegetation (Van de Schootbrugge et al., 2009). Mass extinction at the Triassic-Jurassic boundary is linked to the perturbation of the global carbon cycle within both marine and terrestrial environments (e.g., Pálffy et al., 2001; Hesselbo et al., 2002; Galli et al., 2005, 2007). The amplitude of the negative δ¹³C shift observed at the Triassic-Jurassic boundary ranges from 1.4‰ (Guex et al., 2004; Ward et al., 2007) to 6‰ (Ruhl et al., 2009), making it the largest carbon cycle perturbation of the Mesozoic.

Massive volcanic activity of the Central Atlantic magmatic province closely coincides in time with the mass extinction at the Triassic-Jurassic boundary (Marzoli et al., 1999; Nomade et al., 2007), and it was the most likely trigger for the increased CO₂ fluxes (Hesselbo et al., 2002) considered to be an important factor contributing to the well-documented biotic crisis. Based on paleobotanic evidence, McElwain et al. (1999) calculated a fourfold increase in atmospheric CO₂ across the Triassic-Jurassic boundary. Negative stable carbon isotope excursions recognized at the boundary at several sections worldwide (e.g., Pálffy et al., 2001; Hesselbo et al., 2002; Galli et al., 2005) are considered as evidence for sudden addition of light carbon into oceans and atmosphere. Volcanism is considered as a possible source, but the amplitude of excursions points to additional sources of lighter carbon, e.g., release of methane through dissociation of gas hydrates (Pálffy et al., 2001; Beerling and Berner, 2002). Increased CO₂ fluxes due to Central Atlantic magmatic province volcanism have also been proposed to have caused a major biocalcification crisis at the Triassic-Jurassic

boundary (Hautmann, 2004; Galli et al., 2005). Organisms producing calcareous skeletons would therefore be severely affected, which is in agreement with a conclusion made by Kiessling et al. (2007) that extinction risk at the Triassic-Jurassic boundary was higher for taxa preferring carbonate substrates, especially reef dwellers and taxa preferring onshore settings. A major setback of skeletal carbonate-producing organisms across the Triassic-Jurassic boundary would cause reduction of carbonate production and deposition in both shallow-water platform environments and in deeper-water basinal settings. Even a less drastic scenario, i.e., a change in carbonate production mode due to a decline in skeletal carbonate-producing organisms (e.g., from skeletal to microbial-mediated mud-mound factory; sensu Schlager, 2003), would alter the carbonate depositional system and possibly result in a reduction of carbonate input to the deeper-water environments.

A biocalcification crisis at the Triassic-Jurassic boundary has so far been recognized only in neritic environments. Galli et al. (2005) presented a record from a carbonate-ramp setting of the Southern Alps in northern Italy, where a vast part of the Upper Triassic carbonate ramp was drowned at the Triassic-Jurassic boundary. This is evidenced by a facies change from the thick-bedded coral- and megalodontid-bearing Zu Limestone to thin-bedded micritic limestone of the Malanotte Formation. The facies change occurred contemporaneous with the negative δ¹³C_{carb} excursion and disappearance of the macrofauna and microfauna (Galli et al., 2005). Based on sedimentological, paleontological, and geochemical evidence, Galli et al. (2005) proposed that the ecological crisis, referred to also as biocalcification crisis, was caused by a volcanic CO₂ pulse that reduced calcite supersaturation levels of the end-Triassic oceans on a global scale. A shallow-marine section at St. Audrie's Bay in the United Kingdom also provides evidence of a biocalcification crisis, as characterized by extinction of calcareous nannoplankton and blooms of organic-walled "disaster" species (Van de Schootbrugge et al.,

[†]E-mail: acrne@zrc-sazu.si

2007). Based on reduction of size and replacement of skeletal aragonite by calcite observed in shallow-water epifaunal bivalves, undersaturation of seawater with respect to aragonite and calcite was proposed due to increased fluxes of CO₂ from Central Atlantic magmatic province volcanism (Hautmann, 2004; Hautmann et al., 2008; a more detailed study on the effects on skeletal mineralogy is given in Hautmann, 2006). Berner and Beerling (2007) tested this hypothesis by using a geochemical mass-balance model. They concluded that the amounts of CO₂ and SO₂ degassing to the atmosphere are at the uppermost end of independent estimates, but that these amounts are possible.

Our record from the Budva Basin in Montenegro represents the first documentation of a sudden termination of carbonate deposition across the Triassic-Jurassic boundary in a pelagic environment. Two sections were studied. Stable carbon and oxygen isotopes together with carbonate content were measured from bulk carbonate ($\delta^{13}\text{C}_{\text{carb}}$) and from bulk organic matter ($\delta^{13}\text{C}_{\text{org}}$) across the Triassic-Jurassic boundary defined by radiolarian biostratigraphy, and established carbon isotope curves were compared with data published from other sections. We present data that support the biocalcification crisis hypothesis.

GEOLOGICAL SETTING

The two studied sections, Bar and Čanj, are located in coastal Montenegro, where the Dalmatian zone, Budva zone, and High Karst zone tectonic units are recognized (Figs. 1A and 1B). Both sections are situated within the Budva zone, which paleogeographically corresponded to the northwest-southeast-trending deep-marine Budva Basin, which was bordered

by the Adriatic Carbonate Platform in the southwest and Dinaric Carbonate Platform in the northeast (D'Argenio et al., 1971). The Budva Basin was formed during the Middle Triassic rifting and existed throughout the Mesozoic as the northwest continuation of the Pindos Basin (Fig. 1C). The entire Middle Triassic to Upper Cretaceous succession consists of pelagic sediments (thin-bedded micritic limestones and radiolarian cherts) and intervening carbonate gravity-flow deposits.

The Budva zone consists of several southwest-verging thrust sheets, but in general, a subdivision into a lower and an upper tectonic unit is possible. The Čanj section is located in the lower tectonic unit and was paleogeographically more distal with respect to the Dinaric Carbonate Platform than the Bar section, which is located in the upper tectonic unit. The general stratigraphy from the uppermost Triassic to the mid-Cretaceous and precise location of studied sections are given in Goričan (1994). The relative distance to the carbonate platform was inferred from distribution of resedimented limestones throughout the entire Mesozoic (Goričan, 1994). The most striking difference between the two sections is recorded in the Middle Jurassic: a 220-m-thick Aalenian to Callovian succession composed exclusively of resedimented limestones at the proximal Bar section, which strongly contrasts with the correlative 50-m-thick succession composed of abundant radiolarian chert and shale at the distal Čanj section.

LITHOSTRATIGRAPHY

The Upper Triassic of the Budva Basin is characterized by the Halobia limestone, a white thin-bedded pelagic mudstone with replacement chert occurring as nodules and layers, rare

marl intercalations, and sporadic beds of red siliceous limestone. The Lower Jurassic consists of an ~25-m-thick unit, "Passée Jaspeuse," which consists of red and greenish thin-bedded siliceous limestones alternating with shales. The boundary between the Halobia limestone and the "Passée Jaspeuse" is distinct, easy to recognize, and lithologically similar all over the basin (six sections were studied by Goričan, 1994; see Radiolarian Biostratigraphy for a summary of previous biostratigraphic work) and is therefore interpreted as isochronous in all sections. Two sections, Čanj and Bar, crop out well enough for bed-by-bed sampling.

Čanj Section

At the Čanj section (Figs. 2 and 3), the uppermost part of the Halobia limestone includes pelagic limestones and two 1.7-m-thick and 1-m-thick slumped levels, which were observed 8.25 m and 4.75 m below the lithological boundary; laterally, their thickness and position according to the lithological boundary vary. Very thin marly intercalations within the pelagic mudstones are more common than in the Bar section. Two beds of coarser-grained limestones with micritic clasts of 5 mm in size were recognized, one of which is the last bed of the Halobia limestone. Coarse-grained beds contain intraclasts of radiolarian packstones, clasts with abundant pelagic pelecypods and rare ostracod shells, fragments of echinoderms, brachiopods, and bivalve shells. The lithological contact between the Halobia limestone and the "Passée Jaspeuse" is sharp. The base of the "Passée Jaspeuse" is a 40-cm-thick unit of boundary shales containing two thin beds of calcareous chert and Fe-Mn mineralization. The boundary shales are red, except for the very

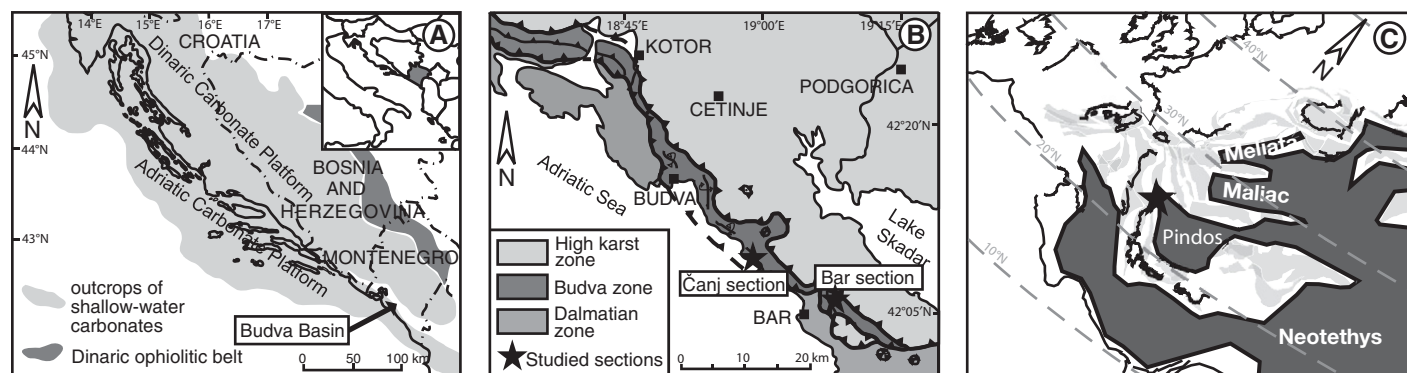


Figure 1. (A) Geographic location of study area, the Budva Basin, with present-day extent of shallow-water carbonates of the Dinaric and Adriatic Carbonate Platforms (modified from Vlahović et al., 2005). (B) Structural map of coastal Montenegro (after Goričan, 1994) with location of studied sections. (C) Paleogeographical reconstruction of the western Tethys around the Triassic-Jurassic boundary (200 Ma) with marked location of the Budva Basin (simplified after Stampfli and Hochard, 2009).



Figure 2. Field photograph of Čanj section. TJB—Triassic-Jurassic boundary.

first layer, which is green. Within the “Passée Jaspeuse,” siliceous limestones alternate with siliceous shales; siliceous limestones are mostly calcisiltites or mudstones to packstones containing radiolarians. A few beds with clasts of siliceous limestones up to a few mm in size are also present; these coarser-grained beds are usually highly silicified. A channelized coarse-grained bed was recognized at 10 m.

Bar Section

The upper part of the Halobia limestone at the Bar section (Fig. 3) consists mostly of thin-bedded pelagic limestones; calcirudites are present only in the uppermost part. The latter mostly contain intraclasts of radiolarian wackestones of up to 1 cm in size; clasts with abundant pelagic pelecypods, individual echinoderm fragments, and ostracod shells are also present. The lithological contact with the overlying siliceous limestones (“Passée Jaspeuse”) is sharp. Within the “Passée Jaspeuse,” most beds are red in color, and only very few—among them also the first beds above the lithological contact—are greenish. The thickness of beds is from less than 1 cm to 15 cm, mostly only a few centimeters. Mudstones, wackestones, and packstones with radiolarians and sponge spicules are by far the most common

facies. Only a few beds are coarser-grained and contain intraclasts of siliceous limestones, which are up to 2 mm in size. A channelized bed was recognized at 6 m.

RADIOLARIAN BIOSTRATIGRAPHY

In a previous biostratigraphic study of the Budva zone (Goričan, 1994), Rhaetian conodonts were extracted from the upper part of the Halobia limestone near Petrovac and Čanj (300 m laterally from the studied section), and Hettangian radiolarians were documented in the lower part of the “Passée Jaspeuse” at Bar and Gornja Lastva. On the basis of these data, it was inferred that the boundary between the two formations corresponded to the Triassic-Jurassic boundary, but the boundary radiolarian faunas were not investigated in detail.

For the present study, all beds where radiolarians were visible in the field with a 20× lens were sampled across a 10 m interval around the lithological boundary. Productive samples are siliceous limestones, which were treated first with acetic (10%) and then with hydrofluoric (5%) acid. In spite of the comparatively poor preservation, the extracted radiolarians allow a reliable distinction between the uppermost Triassic and the lowest Jurassic, because a drastic radiolarian faunal turnover occurs at

the system boundary (Carter and Hori, 2005; Longridge et al., 2007). Characteristic species are illustrated in Figure 4, and their occurrence is given in Table 1. For position of samples, see Figure 3.

Čanj Section

Rhaetian radiolarians were found in samples C 4.43 and C 7.40 of the Čanj section. Both samples are dominated by multicrytid nassellarians. The following species were determined in sample C 4.43: *Bitubopyle cylindrata*, *Canoptum triassicum*, *Globolaxtorum tozeri*, *Laxtorum* cf. *capitaneum*, *Neocanoptum nadanhadense* (*Canoptum* sp. A in Carter, 1993), *Orbiculiformella* sp., *Paronaella* sp., and *Serilla* sp. (*Risella* in Carter, 1993). The most important is *Globolaxtorum tozeri*, which is the index species of the upper Rhaetian *Globolaxtorum tozeri* zone (Carter, 1993). *Serilla*, *Bitubopyle*, as well as medially inflated Canoptidae (*Globolaxtorum*) and Canoptidae with a terminal tube (*Laxtorum capitaneum*, *Neocanoptum*) do not cross the Triassic-Jurassic boundary (Carter, 1993; Longridge et al., 2007; O’Dogherty et al., 2009a). Radiolarians in sample C 7.40 were very poorly preserved, but *Globolaxtorum* and *Laxtorum* cf. *capitaneum* could be identified.

In the “Passée Jaspeuse,” the lowest sample C 8.63 contains predominantly undetermined spherical spumellarians. Nassellarians are extremely rare; *Canoptum merum* and *Droltus hecatensis* were recognized. Both species and the genus *Droltus* first occur in the lowest Hettangian *Canoptum merum* zone (Carter et al., 1998; Longridge et al., 2007). *Pantanellium tanuense*, also first appearing in the *Canoptum merum* zone (Carter et al., 1998), was found in the overlying sample C 9.39.

Bar Section

From the Bar section, only Jurassic radiolarians were recovered. The three samples at the base of the “Passée Jaspeuse” are characterized by different primitive species of spumellarians and entactinarians. Most of them have rod-like rather than bladed spines (Figure 4, V–W, AA–DD). The identified species are: *Charlottea* aff. *weedensis*, *Pantanellium kluense*, *P. tanuense*, *Paronaella ravenensis*, *Thurstonia* cf. *gibsoni*, and *Tipperella* cf. *kennecottensis*. Rings of *Mesosaturnalis*, a survivor genus from the Triassic, have low number of outer spines. *Canoptum* is fairly common but contains only one species, i.e., *Canoptum merum*. The assemblage is assigned to the lower Hettangian *Canoptum merum* zone based on first appearance

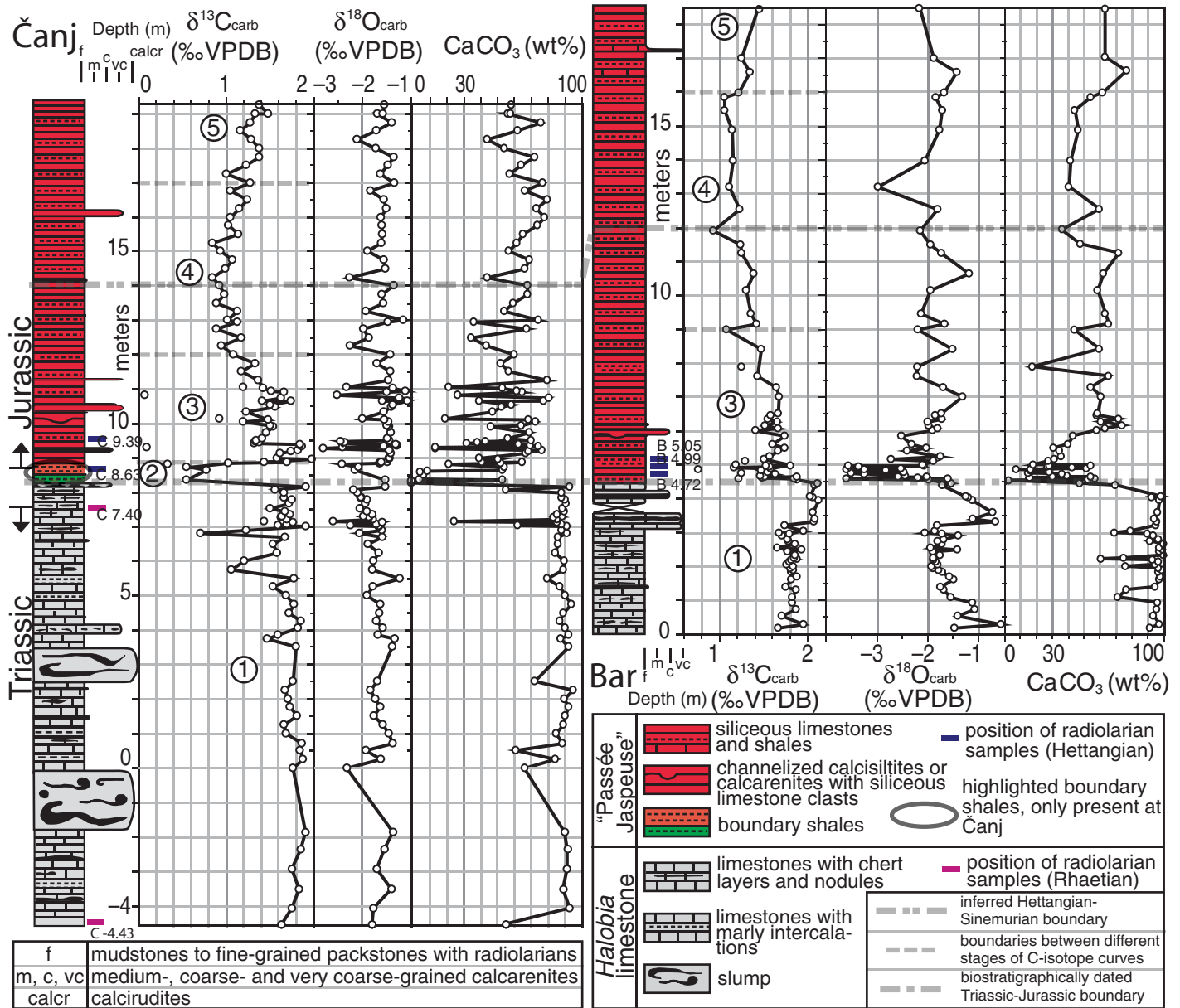


Figure 3. Stratigraphic logs of the studied sections with stable carbon and oxygen isotope curves, carbonate content curves, and marked positions of radiolarian samples (red and blue bars with sample numbers). For intervals of carbon isotope curve (1–5), see text. VPDB—Vienna Pee Dee belemnite.

datums (FADs) of *Canoptum merum*, *Charlottea*, *Pantanellium tanuense*, and *Thurstonia*, and last appearance datum (LAD) of *Tipperella* (Carter et al., 1998; Longridge et al., 2007; O'Dogherty et al., 2009b). Medially broadened multicystids (e.g., *Protokatroma*) that first occur in the successive *Protokatroma aquila* zone were not found. Higher in the section, the radiolarian faunas have not been studied in detail yet. Preliminary observations in sample B 8.05 revealed *Canoptum merum* and spongy spumellarians

with rod-like spines (Spumellarian indet. A of Carter et al., 1998), which do not extend above the middle Hettangian (Carter et al., 1998).

Comparison with Other Radiolarian Localities across the Triassic-Jurassic Boundary

A sudden disappearance of typical Rhaetian taxa and, in the lowest Hettangian, abundance of spherical forms and forms with rod-like spines

are also characteristic patterns of radiolarian faunal change across the Triassic-Jurassic boundary in Queen Charlotte Islands, Canada, and in Japan (Carter and Hori, 2005; Longridge et al., 2007). Outside the circum-Pacific belt, the transition from Rhaetian to Hettangian assemblages is not so precisely documented. Radiolarians have been used to date the Triassic-Jurassic Hocaköy section in Turkey, where the oldest Jurassic radiolarians correspond to the middle-upper Hettangian *Pantanellium browni* zone

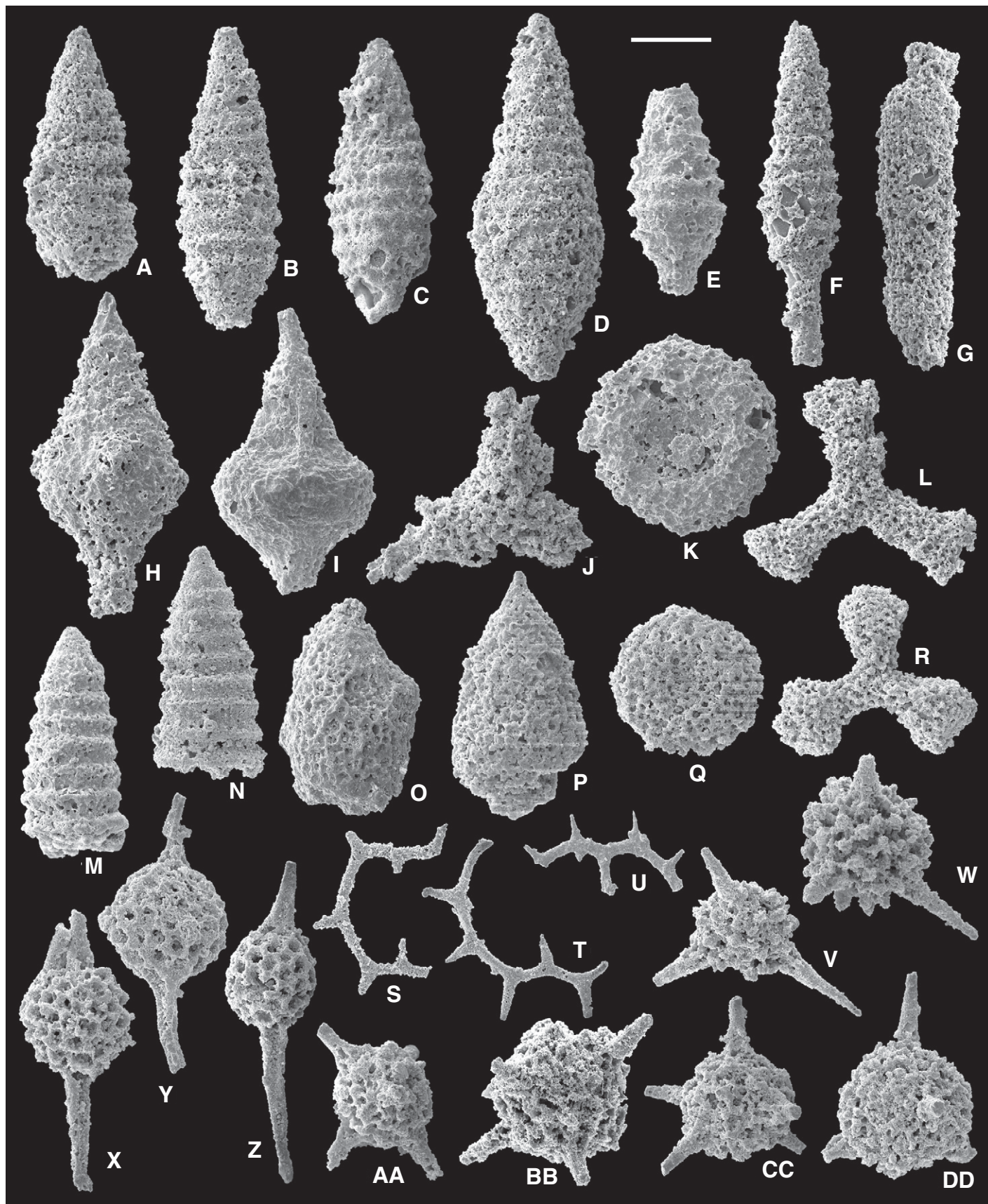


Figure 4.

Figure 4. Radiolarians of the *Globolaxtorum tozeri* zone [(A–L), Čanj section] and *Canoptum merum* zone [Figs. (M–DD), Čanj and Bar sections]. For each illustration the sample number, scanning electron microscope (SEM) number, and magnification (length of scale bar) are indicated. (A) *Canoptum triassicum* Yao, C –4.43, 081626 (scale bar 75 μm). (B–E) *Laxtorum cf. capitaneum* Carter, (B) C –4.43, 081615; (C) C 7.40, 081706; (D) C –4.43, 081601; (E) C 7.40, 081711 (scale bar 75 μm). (F) *Neocanoptum nadanhadense* Zhang, C –4.43, 081613 (scale bar 75 μm). (G) *Bitubopyle cylindrata* (Carter), C –4.43, 081610 (scale bar 100 μm). (H) *Globolaxtorum tozeri* Carter, C –4.43, 081603 (scale bar 75 μm). (I) *Globolaxtorum cf. tozeri* Carter, C 7.40, 081718 (scale bar 75 μm). (J) *Serilla sp.*, C –4.43, 081608 (scale bar 75 μm). (K) *Orbiculiformella sp.*, C 7.40, 081727 (scale bar 100 μm). (L) *Paronaella sp.*, C –4.43, 081629 (scale bar 100 μm). (M–N) *Canoptum merum* Pessagno and Whalen, (M) C 8.63, 081812; (N) B 5.05, 080327 (scale bar 75 μm). (O–P) *Droplitus hecatensis* Pessagno and Whalen, (O) C 8.63, 081814; (P) C 9.39, 081909 (scale bar 75 μm). (Q) *Orbiculiformella sp.*, B 5.05, 080311 (scale bar 100 μm). (R) *Paronaella ravenensis* Whalen and Carter, B 5.05, 080312 (scale bar 100 μm). (S–U) *Mesosaturnalis spp.*, (S) B 4.72, 080102; (T) B 4.99, 080202; (U) C 8.63, 081802 (scale bar 150 μm). (V–W) *Charlottea aff. weedensis* Whalen and Carter, (V) B 4.99, 080215; (W) B 4.72, 080108 (scale bar 75 μm). This species differs from the type material in that the spines are distally circular in cross section. (X–Y) *Pantanellium tanuense* Pessagno and Blome, (X) B 5.05, 080304; (Y) B 4.99, 080210 (scale bar 75 μm). (Z) *Pantanellium kluense* Pessagno and Blome, B 5.05, 080303 (scale bar 75 μm). (AA–CC) *Thurstonia cf. gibsoni* Whalen and Carter, (AA) B 5.05, 080307; (BB) B 4.72, 080118; (CC) B 5.05, 080317 (scale bar 75 μm). (DD) *Tipperella cf. kennecottensis* Carter (in Longridge et al., 2007), B 4.99, 080213 (scale bar 75 μm).

TABLE 1. OCCURRENCE OF CHARACTERISTIC RADIOLARIAN TAXA

Species	Sections Radiolarian zones Samples	Čanj		Bar				
		<i>Globolaxtorum tozeri</i> zone C –4.43	C 7.40	<i>Canoptum merum</i> zone C 8.63	C 9.39	<i>Canoptum merum</i> zone B 4.72	B 4.99	B 5.05
<i>Bitubopyle cylindrata</i> (Carter)		X						
<i>Serilla sp.</i>		X						
<i>Canoptum triassicum</i> Yao		X						
<i>Globolaxtorum tozeri</i> Carter		X	cf.					
<i>Laxtorum cf. capitaneum</i> Carter		X	X					
<i>Neocanoptum nadanhadense</i> Zhang		X						
<i>Orbiculiformella spp.</i>		X	X		X	X	X	X
<i>Paronaella spp.</i>		X				X	X	X
<i>Paronaella ravenensis</i> Whalen and Carter						X	X	X
<i>Canoptum merum</i> Pessagno and Whalen				X		X	X	X
<i>Droplitus hecatensis</i> Pessagno and Whalen				X	X			
<i>Pantanellium tanuense</i> Pessagno and Blome					X	X	X	X
<i>Pantanellium kluense</i> Pessagno and Blome						X	X	X
<i>Mesosaturnalis spp.</i>				X		X	X	X
<i>Charlottea aff. weedensis</i> Whalen and Carter						X	X	
<i>Thurstonia cf. gibsoni</i> Whalen and Carter						X	X	X
<i>Tipperella cf. kennecottensis</i> Carter						X	X	X

(Tekin, 2002). Among other fossils, radiolarians have also been investigated to constrain the Triassic-Jurassic boundary of the Csóvár section in Hungary (Pálffy et al., 2007). In this section, the lowest Jurassic radiolarian assemblage does not contain *Canoptum merum* and is, according to the zonation of Carter et al. (1998), correlated to the interval of the *Protokatroma aquila* to the *Crucella hettangica* zones (Pálffy et al., 2007, p. 19). The early Hettangian radiolarians from the Budva zone thus seem to be the oldest Jurassic radiolarians so far encountered in the Tethyan realm. The studied upper Rhaetian to lower Hettangian succession confirms global correlativity of radiolarian events across the Triassic-Jurassic boundary.

STABLE CARBON ISOTOPES AND CARBONATE CONTENTS

The upper part of the Halobia limestone and the lower part of the “Passée Jaspeuse” were sampled bed-by-bed for geochemical analysis; altogether, 221 samples were analyzed for stable

carbon and oxygen isotopes as well as carbonate content at both sections, and 47 samples were analyzed for stable carbon isotopes in bulk organic matter at Čanj section (GSA Data Repository Table DR¹).

Methods

The isotopic composition of carbonate was measured on bulk rock samples. Approximately 200 μg of powder were reacted with 100% phosphoric acid at 70 °C in a ThermoFisher Kiel IV carbonate device connected to a ThermoFisher Delta V mass spectrometer. The reproducibility of the measurements based on replicated standards was $\pm 0.02\text{‰}$ for $\delta^{13}\text{C}$ and $\pm 0.06\text{‰}$ for $\delta^{18}\text{O}$. The instrument was calibrated with the international standards NBS19 and NBS18. The isotope values are reported in the conventional

delta notation with respect to Vienna Pee Dee belemnite (VPDB).

The isotopic composition of organic matter was measured on decarbonated bulk rock samples. Samples were treated with 2 M HCl and left for a minimum of 12 h as long as there was no more visible reaction (at least three times). The residues were rinsed several times with distilled water, dried for 48 h at 60 °C, and homogenized in an agate mortar. Because six samples repeatedly exhibited extremely high values (from -18‰ to -23‰), we suspected that traces of poorly soluble carbonate, e.g., siderite, were still present within the samples. We therefore repeated the process of carbonate removal on all samples, using 12 M HCl, and left them overnight. Most of the samples with compositions lower than -26‰ did not show significant changes in $\delta^{13}\text{C}$ (average change was -0.22‰), whereas the overall average change in isotope values after carbonate removal by the 12 M HCl was -0.92‰ , but the overall pattern remained the same. However, even after these treatments, three samples

¹GSA Data Repository item 2010135, Stable carbon and oxygen isotope data together with wt% CaCO_3 contents, is available at <http://www.geosociety.org/pubs/ft2010.htm> or by request to editing@geosociety.org.

continued to exhibit rather high $\delta^{13}\text{C}_{\text{org}}$ values (-22.5‰ and -24.5‰ ; see Fig. 5).

For isotope measurements of organic matter, a few milligrams of decarbonated powder were weighted in tin capsules and measured using a ThermoFisher Flash-EA coupled to a Delta V mass spectrometer. The reproducibility of the measurements based on replicated standards was $\pm 0.1\text{‰}$ for $\delta^{13}\text{C}$. The instrument was calibrated with the international standards NBS22 and IAEA-CH-6, and the isotope values are reported in the conventional delta notation with respect to VPDB.

Carbonate Content Data

At both sections, the vast majority of Halobia limestone beds contains more than 80% of CaCO_3 ; the average carbonate content is 89% at Bar and 84% at Čanj. Across the lithological boundary, the carbonate content falls abruptly; at Čanj, 6 out of 8 samples within the boundary shales contain less than 10% of CaCO_3 . Within the “Passée Jaspeuse” of both sections, carbonate content ranges from 15% to 80%. The $\delta^{13}\text{C}_{\text{carb}}$ value of samples with very low carbonate contents ($10\% < \text{CaCO}_3 \leq 30\%$) at Čanj

section, where isotopes and wt% CaCO_3 were analyzed bed-by-bed, is on average 1.0‰ lower than the carbonate-rich ($\text{CaCO}_3 \geq 50\%$) beds immediately below and above these samples (excluding the boundary shales, as these might reflect lower $\delta^{13}\text{C}$ values due to changes in seawater composition) (Fig. 6A). This suggests that samples with low carbonate have been altered by diagenesis. The range of the $\delta^{13}\text{C}_{\text{carb}}$ variability estimated for samples with carbonate content between 10% and 30% is from 0.2‰ to 2.5‰ , while almost no difference is observed (0.2‰) for samples with a carbonate content between 30% and 40% (Fig. 6A). Samples of both siliceous limestones and marls with CaCO_3 content less than 30% yielded much lower values of $\delta^{13}\text{C}_{\text{carb}}$, and a few of them also had very low values of $\delta^{18}\text{O}_{\text{carb}}$ (Fig. 6B). Shales and siliceous limestones that contained more than 30% of CaCO_3 yielded $\delta^{13}\text{C}_{\text{carb}}$ values similar to the carbonate-rich beds above and below them. Additionally, while there is no correlation between $\delta^{13}\text{C}_{\text{carb}}$ and wt% CaCO_3 for samples with high carbonate content, a correlation between $\delta^{13}\text{C}_{\text{carb}}$ and wt% CaCO_3 exists for samples containing less than 30% of CaCO_3 (Fig. 6C), which reflects probable diagenetic overprint of carbonate-poor

samples. For this reason, we excluded samples with less than 30% carbonate when plotting the $\delta^{13}\text{C}_{\text{carb}}$ curve. The $\delta^{18}\text{O}_{\text{carb}}$ of all samples shown on the $\delta^{13}\text{C}_{\text{carb}}$ curve is relatively stable, between -3.5‰ and -0.5‰ (VPDB) (Figs. 3 and 6B). It is important to point out that all four samples with lower $\delta^{13}\text{C}_{\text{carb}}$ values at the beginning of the “Passée Jaspeuse” at Čanj contain more than 50% of CaCO_3 and yield normal marine values of $\delta^{18}\text{O}_{\text{carb}}$ (Fig. 3; samples marked with asterisk in Figs. 6B and 6C), and this rules out a major diagenetic overprint.

Stable Carbon Isotope Data

Five main stages of the evolution of the stable carbon isotope record were distinguished (Fig. 3; four stages shown in Fig. 5). Within the first stage (1 in Fig. 3), $\delta^{13}\text{C}_{\text{carb}}$ values fluctuate around 1.8‰ (VPDB) in the Upper Triassic Halobia limestone in both studied sections, and $\delta^{13}\text{C}_{\text{org}}$ values fluctuate around -26.5‰ in the Upper Triassic at Čanj section (Fig. 5). The Čanj curve is characterized by three short excursions in $\delta^{13}\text{C}_{\text{carb}}$ to more negative values, which were not identified at the Bar section.

The second stage (2 in Fig. 3; main negative carbon isotope excursion [CIE] in Fig. 5) corresponds to the “negative spike,” which is defined as a shift with the largest amplitude measured in both bulk carbonate (1.3‰) and bulk organic matter (1.1‰), and which is positioned within the very first beds of the “Passée Jaspeuse; the first two samples with lower $\delta^{13}\text{C}_{\text{carb}}$ values are within the “boundary shales,” and all lower $\delta^{13}\text{C}_{\text{org}}$ samples, except for one (at 8.87 m), occur within the “boundary shales.” The most probable explanation for the absence of the negative spike at a more proximal Bar section, where boundary shales are absent, is a stratigraphic gap; shales were probably only deposited in the distal part of the Budva Basin.

The third stage of the stable carbon isotope record (3 in Fig. 3) corresponds to shifts toward higher $\delta^{13}\text{C}$ values. Immediately following the negative shift at Čanj, $\delta^{13}\text{C}_{\text{carb}}$ reaches the maximum value (2.0‰) of all studied samples within the “Passée Jaspeuse”; further up section, two to three shifts toward heavier $\delta^{13}\text{C}$ values can be distinguished (a, b_1 , b_2 in Fig. 5). A slow decrease of $\delta^{13}\text{C}_{\text{carb}}$ from 1.8‰ to lower values around 1.2‰ is clearly seen at both sections and represents the last part of the third stage in the evolution of the stable carbon isotope record. In the lower part of the third stage of the $\delta^{13}\text{C}_{\text{org}}$ record, rather high $\delta^{13}\text{C}_{\text{org}}$ values (-22.5‰ and -24.5‰) were measured in three samples (marked as triangles in Fig. 5). As these values are exceptionally high (see Methods section) and are not confirmed by at least

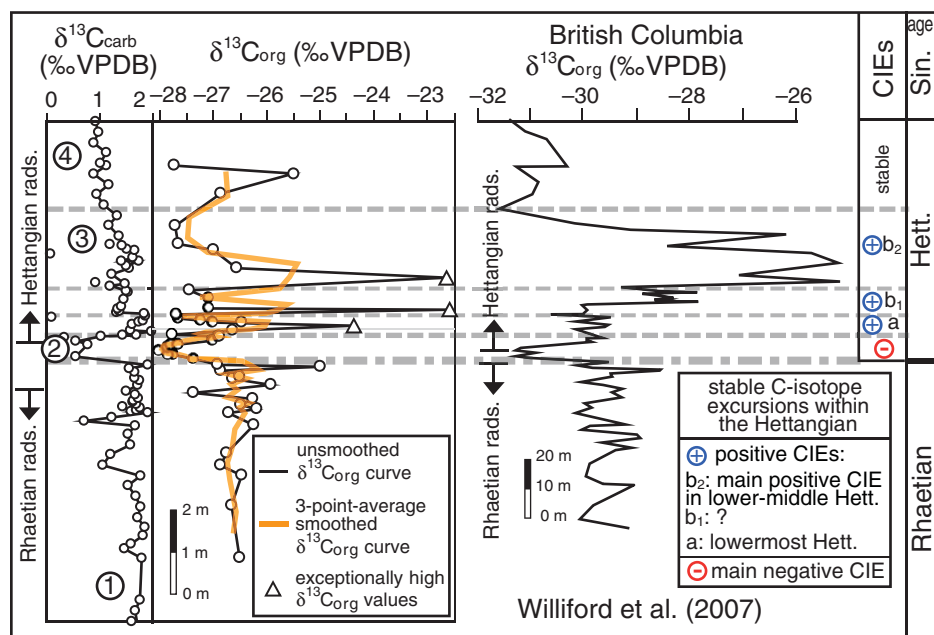


Figure 5. Stable carbon isotope curves for bulk carbonate ($\delta^{13}\text{C}_{\text{carb}}$) and bulk organic matter ($\delta^{13}\text{C}_{\text{org}}$) from Čanj section and comparison with stable carbon isotope curve from bulk organic matter in British Columbia (Williford et al., 2007). The Triassic-Jurassic boundary of both sections is precisely dated with radiolarians. The Hettangian-Sinemurian boundary at Čanj (14 m) is based on stable carbon isotope correlations. The tops of both sections, Čanj and Queen Charlotte Islands in British Columbia (Williford et al., 2007), correspond to the Hettangian-Sinemurian boundary. CIE—carbon isotope excursion; VPDB—Vienna Peedee belemnite.

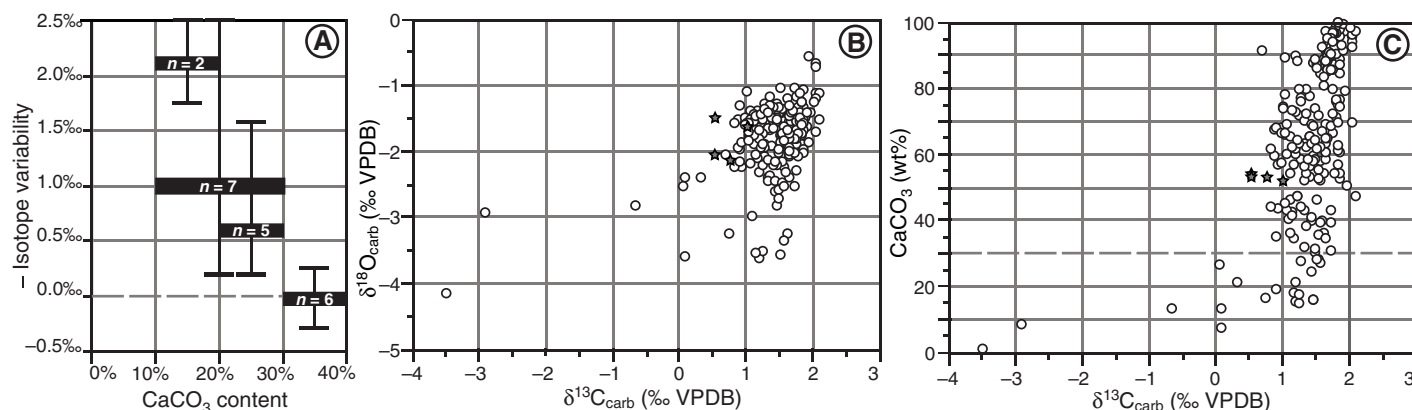


Figure 6. (A) $\delta^{13}\text{C}_{\text{carb}}$ variability of successive samples (excluding the boundary shales) plotted against the carbonate content; the black rectangle is positioned at the average $\delta^{13}\text{C}_{\text{carb}}$ variability of the successive samples (the number in white shows the number of samples); the range of the $\delta^{13}\text{C}_{\text{carb}}$ variability is also shown. Samples with $30\% < \text{wt}\% \text{CaCO}_3 \leq 40\%$ have a range of $\delta^{13}\text{C}_{\text{carb}}$ variability from -0.26‰ to $+0.28\text{‰}$, which makes an average $\delta^{13}\text{C}_{\text{carb}}$ variability of zero. (B) Cross-plotted values of $\delta^{18}\text{O}_{\text{carb}}$ and $\delta^{13}\text{C}_{\text{carb}}$ (all samples). (C) Carbonate content plotted against $\delta^{13}\text{C}_{\text{carb}}$ (all samples). Stars (B, C) mark the samples exhibiting low $\delta^{13}\text{C}_{\text{carb}}$ values with carbonate content above 50% at the beginning of the “Passée Jaspeuse.” VPDB—Vienna Peedee belemnite.

two consecutive samples, we cannot be sure that the three very positive samples represent a reliable record across the Triassic-Jurassic boundary.

The fourth stage in the evolution of the stable carbon isotope record shows stable values in $\delta^{13}\text{C}_{\text{carb}}$: around 1.0‰ at Čanj and 1.2‰ at Bar (4 in Fig. 3). The beginning of the fifth stage (5 in Fig. 3) is placed where $\delta^{13}\text{C}_{\text{carb}}$ values start climbing toward higher values.

DISCUSSION

At both studied sections in the Budva Basin, the Triassic-Jurassic boundary is placed at the lithological transition between the Halobia limestone and “Passée Jaspeuse” on the basis of radiolarian biostratigraphy. The negative spike in the stable carbon isotope curve, measured in bulk carbonate and bulk organic matter, is recognized in the very first beds of the “Passée Jaspeuse” and occurs simultaneously with the rapid drop in carbonate content from more than 80% to less than 10%. The prominent facies change from pelagic limestones to carbonate-poor siliceous deposits indicates an abrupt reduction of carbonate deposition in the basin, and it is contemporaneous with the negative anomaly of more than 1‰ in the stable carbon isotope record. This lithological change in the Budva Basin can be biostratigraphically correlated to the facies change on the margin of the Dinaric Carbonate Platform, where the thick-bedded Upper Triassic Dachstein limestone with abundant Rhaetian fauna is overlain by medium-bedded Lower Jurassic micritic limestones containing almost exclusively

peloids and only rare foraminifers (Črne and Goričan, 2008). The facies change from thick-bedded shallow-water Dachstein limestone into micritic limestone marks the drowning of the southwestern part of the Dinaric carbonate platform at the Triassic-Jurassic boundary (Črne and Goričan, 2008).

Correlations with Other Triassic-Jurassic Boundary Successions: Facies Change and Stable C-Isotope Record

The sections from the Budva Basin represent the deepest-marine successions with detailed biostratigraphic and stable carbon isotope data. Both biostratigraphy and geochemistry enable us to correlate the sections in the Budva Basin to other sections containing the Triassic-Jurassic boundary (Fig. 7). Facies change from the thick-bedded coral and megalodontid-bearing Zu Limestone (Zu-3 member) to thin-bedded micritic limestone of the Malanotte Formation in the Southern Alps in northern Italy is contemporaneous with the negative excursion in $\delta^{13}\text{C}_{\text{carb}}$ (Galli et al., 2005, 2007). Additionally, an abrupt lithological change from basinal carbonates of the Kössen Formation to marls and clayey sediments of the lower Kendlbach Formation of the Northern Calcareous Alps (Austria) also occurs simultaneously with a negative excursion in $\delta^{13}\text{C}_{\text{org}}$ (Kürschner et al., 2007; Von Hillebrandt et al., 2007; Ruhl et al., 2009). Furthermore, a sharp lithological boundary between the shallow-water Fatra Formation and lower Hettangian deeper-marine marls of the Kopianec Formation in the Zliechov Basin of the Western Carpathians (Poland and Slo-

vakia) marks a sudden termination of carbonate deposition and also exhibits a negative $\delta^{13}\text{C}_{\text{carb}}$ anomaly (Michalík et al., 2007). Our record of $\delta^{13}\text{C}_{\text{carb}}$ also correlates well with the record of St. Audrie’s Bay (UK; Hesselbo et al., 2002), where the “initial isotope excursion” corresponds to the negative excursion in the record of the Budva Basin (Fig. 7). At the Csóvár section (Hungary), a distinct layer corresponding to the “boundary-event horizon” lies within the laminated turbidites and radiolarian wackestones and corresponds to the principal negative $\delta^{13}\text{C}_{\text{carb}}$ excursion (Pálffy et al., 2007). While the Csóvár section is easily correlative to the Budva Basin on the basis of the negative $\delta^{13}\text{C}_{\text{carb}}$ anomaly, there is no prominent facies change across the boundary at the Csóvár section; the facies change from medium- to fine-grained calciturbidites into laminated calcisiltites occurs several meters below the boundary-event horizon. This comparison of various stable carbon isotope records with our new sections, however, clearly indicates that the negative carbon isotope anomaly reflects a perturbation of the global carbon cycle. The negative anomaly is recognized in bulk organic matter and bulk carbonates; the latter cannot be explained by changes in relative contributions of different sources, as was postulated to explain negative excursions measured in organic matter by Van de Schootbrugge et al. (2008). The contemporaneous negative anomaly measured in both bulk carbonates and bulk organic matter therefore corroborates the hypothesis of a change in the isotope composition of the global exogenic carbon reservoir (e.g., Pálffy et al., 2001; Hesselbo et al., 2002; Galli et al., 2005).

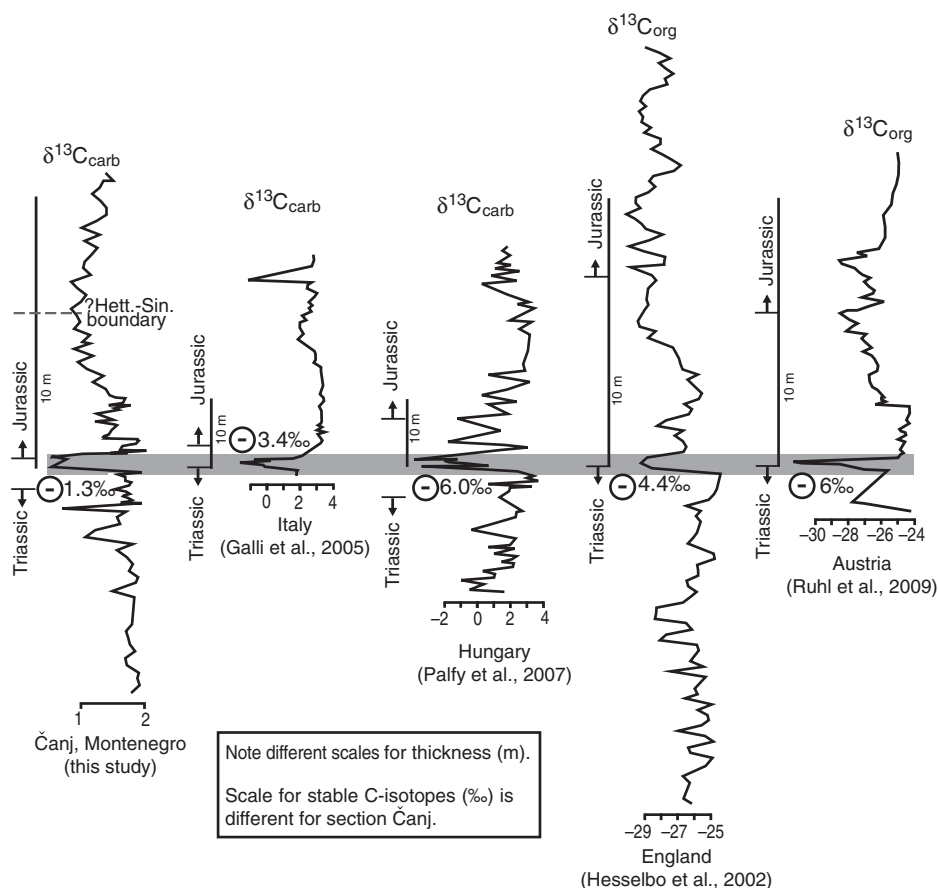


Figure 7. Correlations of carbon isotope curve from Čanj section to other carbon isotope curves across the Triassic-Jurassic boundary with marked amplitudes of negative stable carbon isotope excursions. The amplitudes of stable carbon isotope excursions were measured from the cited references. Last occurrence of Triassic and first occurrence of Jurassic fossils together with a 10 m scale bar are indicated on the left side of each curve.

The negative shift in the Budva Basin (1.3‰ in $\delta^{13}\text{C}_{\text{carb}}$ and 1.1‰ $\delta^{13}\text{C}_{\text{org}}$) represents the shift with the smallest amplitude recognized so far in Triassic-Jurassic boundary sections; the range of negative shifts elsewhere is between 1.4‰ (Nevada, United States: Guex et al., 2004; Ward et al., 2007) and 6‰ (Austria: Von Hillebrandt et al., 2007; Ruhl et al., 2009). The record from the Budva Basin represents the deepest-marine record of all Triassic-Jurassic boundary sections studied so far. Depletion of $\delta^{13}\text{C}_{\text{carb}}$ due to excessive evaporation or freshwater influx common in shallow-water settings, therefore, cannot be used to explain the low $\delta^{13}\text{C}_{\text{carb}}$ values at the Triassic-Jurassic boundary in the Budva Basin. Furthermore, the amplitude of the negative spike is almost the same in both bulk carbonate and bulk organic matter. We suggest that the record from the Budva Basin may therefore represent the $\delta^{13}\text{C}$ negative shift with the most reliable amplitude. We are aware, however, that it is also possible that the smaller amplitude of the negative

$\delta^{13}\text{C}_{\text{carb}}$ shift was a consequence of either lower input of carbonate and/or increased dissolution, causing lower sedimentation rates of carbonate exactly at the Triassic-Jurassic boundary. Such an effect has been documented in deep, open-ocean settings across the Paleocene-Eocene thermal maximum, where stable carbon isotope records at paleodepths of 1500 m show an isotope excursion of -3.5‰ , but only -1.5‰ at 3600 m (McCarren et al., 2008). A smaller shift in the deep-marine locations was interpreted by McCarren et al. (2008) to be a consequence of a truncation of the stratigraphic record in the deep-marine environments due to ocean acidification and widespread dissolution of carbonates. A similar scenario could also be applicable across the Triassic-Jurassic boundary.

A detailed biostratigraphy of the whole “Passeé Jaspeuse” is beyond the scope of this paper, but the presented radiolarian biostratigraphy confirms the presence of at least 3.5 m of Hettangian sediments. Goričan (1994) reported a

late Sinemurian radiolarian fauna 24 m above the lithological contact at Bar section. Based on previously reported stable $\delta^{13}\text{C}_{\text{carb}}$ (Van de Schootbrugge et al., 2008) and $\delta^{13}\text{C}_{\text{org}}$ (Williford et al., 2007) records across the Hettangian-Sinemurian boundary, we conclude that the Hettangian-Sinemurian boundary corresponds to a level around 14 m at Čanj section and 12 m at Bar section (Fig. 3). A total thickness of Hettangian sediments would be therefore 5.5 m at Čanj and 7.5 m at Bar. Considering the duration of the Hettangian stage as less than 2 m.y. (Schaltegger et al., 2008), the sedimentation rate for the Hettangian siliceous limestones alternating with shales is around 3–4 m/m.y., which is normal when compared with younger chert of the same basin (1.5–2 m/m.y.; calculated for Middle and Upper Jurassic radiolarites by Goričan, 1994), or even high when compared with Lower Jurassic cherts of an open oceanic realm (1.2 m/m.y.; Hori et al., 1993). Pelagic sections appear condensed when compared to neritic sections. By comparing our pelagic sedimentation rates in the lowermost Jurassic with other pelagic records of the same age, we have shown that the sedimentation rates in the Budva Basin were quite high for a pelagic realm. Our record could therefore be one of the more complete pelagic records across the Triassic-Jurassic boundary. Because massive Central Atlantic magmatic province volcanic activity closely coincides in time with the Triassic-Jurassic boundary (Marzoli et al., 1999; Nomade et al., 2007), we interpret the negative $\delta^{13}\text{C}$ excursion as a consequence of volcanic eruptions. However, as larger amplitudes of negative $\delta^{13}\text{C}$ excursion have been recognized within other sections across Europe (e.g., Pálffy et al., 2001; Galli et al., 2005; Ruhl et al., 2009), additional sources of light carbon, e.g., release of methane through dissociation of gas hydrates (Pálffy et al., 2001; Beerling and Berner, 2002), are also possible. We also note the presence of three negative anomalies of smaller amplitude in the $\delta^{13}\text{C}_{\text{carb}}$ record preceding the main negative spike. They could be considered as evidence for multiple volcanic pulses at the very end of the Rhaetian, although their significance has to be confirmed from other sections.

A positive anomaly was recognized in the lower-middle Hettangian $\delta^{13}\text{C}_{\text{org}}$ record of the British Columbia (Williford et al., 2007; Fig. 5). We tentatively correlate the large positive anomaly of the early Hettangian reported by Williford et al. (2007) with three positive anomalies identified in the $\delta^{13}\text{C}_{\text{carb}}$ and $\delta^{13}\text{C}_{\text{org}}$ record of the Budva Basin (a, b in Fig. 5). Since the sedimentation rates in the pelagic Budva Basin were low in comparison to other Hettangian records (see Fig. 7), we cannot exclude

that gaps, not recognized in the biostratigraphy, explain the noisy record in the Hettangian part of the succession. It is difficult to confirm with certainty that the “positive anomalies” recognized in the Budva Basin are correlatable with other Hettangian positive excursions recognized in $\delta^{13}\text{C}$ records (Williford et al., 2007; Van de Schootbrugge et al., 2008) because the large amplitudes of positive excursions in our $\delta^{13}\text{C}_{\text{org}}$ record are supported only by single data points. Measurements of $\delta^{13}\text{C}$ in fully pelagic Hettangian successions around the world would help to solve this problem.

Scenarios for Carbonate Decrease across the Triassic-Jurassic Boundary in the Budva Basin

The abrupt reduction of carbonate content in the Budva Basin occurred contemporaneous with a negative anomaly in the stable carbon isotope record. Possible nonexclusive scenarios for a sudden decrease of carbonate content are: (1) shoaling of the calcite compensation depth (CCD) due to acidification of the ocean (similar to that postulated for the Paleocene-Eocene thermal maximum; Zachos et al., 2005); (2) reduced carbonate production due to a biocalcification crisis and consequently reduced input of shallow-water carbonate into the deep basin, caused by undersaturation of the ocean with respect to CaCO_3 (e.g., in the Cretaceous; Wissler et al., 2003); and (3) a change in the carbonate production mode, e.g., from tropical to microbially mediated mud-mound factory (sensu Schlager, 2003), which would have led to reduced shedding of shallow-water carbonates into the basin. Acidification of the ocean (Hautmann et al., 2008) as a result of increased fluxes of CO_2 , SO_2 , and CH_4 at the Triassic-Jurassic boundary is possible (Bernier and Beerling, 2007) and provides two mechanisms resulting in the reduction of CaCO_3 in pelagic settings: (1) enhanced dissolution of carbonate (shoaling of the CCD); and (2) lower carbonate input due to the choking of carbonate producers in neritic environments (e.g., Orr et al., 2005). A change to a microbially dominated carbonate production could be the result of the widespread ecological collapse (Schlager, 2003). A comparable change occurred at the Permian-Triassic boundary, when the skeletal carbonate factory was abruptly replaced by a microbial community (e.g., Baud et al., 2007). If a biocalcification crisis is defined as a crisis of skeletal carbonate-producing organisms, both a decline of carbonate production in shallow-water environments and a change in carbonate production mode can be considered as a biocalcification crisis sensu lato.

As already discussed under Correlations with Other Triassic-Jurassic Boundary Successions, important facies changes across the Triassic-Jurassic boundary are known from other sections, covering a variety of depositional environments (a summary of lithological changes across the Triassic-Jurassic boundary is given in fig. 1 in Hautmann et al., 2008). The most common facies change corresponds to carbonate platform drowning (Galli et al., 2005, 2007; Michalík et al., 2007; Črne and Goričan, 2008), but lithological change is also known from the basinal environment (Kürschner et al., 2007; Von Hillebrandt et al., 2007; Ruhl et al., 2009; this study). While shoaling of the CCD would affect only deep-marine environments, a biocalcification crisis could explain the facies change in different depositional settings.

Enhanced dissolution of carbonate (shoaling of the CCD) and a biocalcification crisis remain the two possible scenarios for an abrupt drop in carbonate content in pelagic settings. The biocalcification crisis is a more probable scenario because important facies changes occurred across the Triassic-Jurassic boundary in a variety of depositional environments. Possible amplifiers of this facies change in the Budva Basin include: (1) increased rate of tectonic subsidence, which is supported by occurrence of slumps in the Upper Triassic pelagic Halobia limestone; (2) relative sea-level rise, recognized in the earliest Jurassic of numerous sections (e.g., Hallam, 1997); and (3) possible gap at the lithological boundary (?uppermost Rhaetian), which would emphasize the observed abruptness of the decrease in both CaCO_3 and $\delta^{13}\text{C}_{\text{carb}}$.

CONCLUSION

The Triassic-Jurassic boundary in the pelagic sediments of the Budva Basin is biostratigraphically constrained with radiolarians. Faunal changes across the system boundary are comparable to those recognized in Queen Charlotte Islands and in Japan. An abrupt reduction of carbonate content observed across the Triassic-Jurassic boundary occurred contemporaneous with a negative anomaly in the stable carbon isotope record. This is considered to be a result of accelerated carbonate dissolution, causing shoaling of the calcium compensation depth, or more probably as a product of reduced carbonate input due to a biocalcification crisis sensu lato, which includes a change in the carbonate production mode, e.g., from skeletal to microbial. Both scenarios are compatible with increased CO_2 , SO_2 , and CH_4 fluxes due to Central Atlantic magmatic province volcanism causing undersaturation of ocean with respect to calcium carbonate.

ACKNOWLEDGMENTS

This study was supported financially by the Slovenian Research Agency, project number P1-0008, and by an Ad futura grant to Črne. We are much obliged to Maya Elrick, Elizabeth S. Carter, Jean Guex, and anonymous reviewers for critical reading of the manuscript and valuable suggestions. We are grateful to Andrej Šmuc, Tom Popit, Jadranka Kurtić, Boštjan Rožič, and Miloš Bartol for all the help with field work. We are thankful to Maria Coray Strasser and Thomas Schmid for assistance in the isotope laboratory, to Christina Keller and Irene Brunner for their efforts concerning the Coulomat, and to Kata Cvetko-Barić for preparation of thin sections.

REFERENCES CITED

- Bambach, R.K., 2006, Phanerozoic biodiversity mass extinctions: Annual Review of Earth and Planetary Sciences, v. 34, p. 127–155, doi: 10.1146/annurev.earth.33.092203.122654.
- Baud, A., Richo, S., and Pruss, S., 2007, The Lower Triassic anachronistic carbonate facies in space and time: Global and Planetary Change, v. 55, p. 81–89, doi: 10.1016/j.gloplacha.2006.06.008.
- Beerling, D.J., and Berner, R.A., 2002, Biogeochemical constraints on the Triassic-Jurassic boundary carbon cycle event: Global Biogeochemical Cycles, v. 16, p. 1036, doi: 10.1029/2001GB001637.
- Berner, R.A., and Beerling, D.J., 2007, Volcanic degassing necessary to produce a CaCO_3 undersaturated ocean at the Triassic-Jurassic boundary: Palaeogeography, Palaeoclimatology, Palaeoecology, v. 244, p. 368–373, doi: 10.1016/j.palaeo.2006.06.039.
- Carter, E.S., 1993, Biochronology and paleontology of uppermost Triassic (Rhaetian) radiolarians, Queen Charlotte Islands, British Columbia, Canada: Mémoires de Géologie (Lausanne), v. 11, p. 1–175.
- Carter, E.S., and Hori, R.S., 2005, Global correlation of the radiolarian faunal change across the Triassic-Jurassic boundary: Canadian Journal of Earth Sciences, v. 42, p. 777–790, doi: 10.1139/e05-020.
- Carter, E.S., Whalen, P.A., and Guex, J., 1998, Biochronology and paleontology of Lower Jurassic (Hettangian and Sinemurian) radiolarians, Queen Charlotte Islands, British Columbia: Geological Survey of Canada, Bulletin, v. 496, p. 1–162.
- Črne, A.E., and Goričan, Š., 2008, The Adriatic-Dinaric carbonate platform margin in the Early Jurassic: A comparison between successions in Slovenia and Montenegro: Bollettino della Società Geologica Italiana, v. 127, p. 389–405.
- D’Argenio, B., Radoičić, R., and Sgroso, I., 1971, A paleogeographic section through the Italo-Dinaric external zones during Jurassic and Cretaceous times: Nafta, v. 22, p. 195–207.
- Galli, M.T., Jadoul, F., Bernasconi, S.M., and Weissert, H., 2005, Anomalies in global carbon cycling and extinction at the Triassic-Jurassic boundary: Evidence from a marine C-isotope record: Palaeogeography, Palaeoclimatology, Palaeoecology, v. 216, p. 203–214, doi: 10.1016/j.palaeo.2004.11.009.
- Galli, M.T., Jadoul, F., Bernasconi, S.M., Cirilli, S., and Weissert, H., 2007, Stratigraphy and palaeoenvironmental analysis of the Triassic-Jurassic transition in the western southern Alps (Northern Italy): Palaeogeography, Palaeoclimatology, Palaeoecology, v. 244, p. 52–70, doi: 10.1016/j.palaeo.2006.06.023.
- Goričan, Š., 1994, Jurassic and Cretaceous radiolarian biostratigraphy and sedimentary evolution of the Budva zone (Dinarides, Montenegro): Mémoires de Géologie (Lausanne), v. 18, p. 1–177.
- Guex, J., Bartolini, A., Atudorei, V., and Taylor, D., 2004, High-resolution ammonite and carbon isotope stratigraphy across the Triassic-Jurassic boundary at New York Canyon (Nevada): Earth and Planetary Science Letters, v. 225, p. 29–41, doi: 10.1016/j.epsl.2004.06.006.
- Hallam, A., 1997, Estimates of the amount and rate of sea-level change across the Rhaetian-Hettangian

- and Pliensbachian-Toarcian boundaries (latest Triassic to early Jurassic): *Journal of the Geological Society of London*, v. 154, p. 773–779, doi: 10.1144/gsjgs.154.5.0773.
- Hautmann, M., 2004, Effect of end-Triassic CO₂ maximum on carbonate sedimentation and marine mass extinction: *Facies*, v. 50, p. 257–261, doi: 10.1007/s10347-004-0020-y.
- Hautmann, M., 2006, Shell mineralogical trends in epifaunal Mesozoic bivalves and their relationship to seawater chemistry and atmospheric carbon dioxide concentration: *Facies*, v. 52, p. 417–433, doi: 10.1007/s10347-005-0029-x.
- Hautmann, M., Benton, M.J., and Tomašových, A., 2008, Catastrophic ocean acidification at the Triassic-Jurassic boundary: *Neues Jahrbuch für Geologie und Paläontologie—Abhandlungen*, v. 249, p. 119–127.
- Hesselbo, S.P., Robinson, S.A., Surlyk, F., and Piasecki, S., 2002, Terrestrial and marine extinction at the Triassic-Jurassic boundary synchronized with major carbon-cycle perturbation: A link to initiation of massive volcanism?: *Geology*, v. 30, p. 251–254, doi: 10.1130/0091-7613(2002)030<0251:TAMEAT>2.0.CO;2.
- Hori, R.S., Cho, C.F., and Umeda, H., 1993, Origin of cyclicity in Triassic-Jurassic radiolarian bedded cherts of the Mino accretionary complex from Japan: *The Island Arc*, v. 3, p. 170–180.
- Kiessling, W., Aberhan, M., Brenneis, B., and Wagner, P.J., 2007, Extinction trajectories of benthic organisms across the Triassic-Jurassic boundary: *Palaeogeography, Palaeoclimatology, Palaeoecology*, v. 244, p. 201–222, doi: 10.1016/j.palaeo.2006.06.029.
- Kürschner, W.M., Bonis, N.R., and Krystyn, L., 2007, Carbon-isotope stratigraphy and palynostratigraphy of the Triassic-Jurassic transition in the Tiefengraben section, northern calcareous Alps (Austria): *Palaeogeography, Palaeoclimatology, Palaeoecology*, v. 244, p. 257–280, doi: 10.1016/j.palaeo.2006.06.031.
- Longridge, L.M., Carter, E.S., Smith, P.L., and Tipper, H.W., 2007, Early Hettangian ammonites and radiolarians from the Queen Charlotte Islands, British Columbia, and their bearing on the definition of the Triassic-Jurassic boundary: *Palaeogeography, Palaeoclimatology, Palaeoecology*, v. 244, p. 142–169, doi: 10.1016/j.palaeo.2006.06.027.
- Marzoli, A., Renne, P.R., Piccirillo, E.M., Ernesto, M., Bellieni, G., and De Min, A., 1999, Extensive 200-million-year-old continental flood basalts of the Central Atlantic magmatic province: *Science*, v. 284, p. 616–618, doi: 10.1126/science.284.5414.616.
- McCarren, H., Thomas, E., Hasegawa, T., Röhl, U., and Zachos, J.C., 2008, Depth dependency of the Paleocene-Eocene carbon isotope excursion: Paired benthic and terrestrial biomarker records (Ocean Drilling Program Leg 208, Walvis Ridge): *Geochemistry, Geophysics, Geosystems*, v. 9, p. Q10008, doi: 10.1029/2008GC002116.
- McElwain, J.C., Beerling, D.J., and Woodward, F.I., 1999, Fossil plants and global warming at the Triassic-Jurassic boundary: *Science*, v. 285, p. 1386–1390, doi: 10.1126/science.285.5432.1386.
- McGhee, G.R., Jr., Sheehan, P.M., Bottjer, D.J., and Droser, M.L., 2004, Ecological ranking of Phanerozoic biodiversity crisis: Ecological and taxonomic severities are decoupled: *Palaeogeography, Palaeoclimatology, Palaeoecology*, v. 211, p. 289–297, doi: 10.1016/j.palaeo.2004.05.010.
- Michalík, J., Lintnerová, O., Gaždžicki, A., and Soták, J., 2007, Record of environmental changes in the Triassic-Jurassic boundary interval in the Zliechov Basin, Western Carpathians: *Palaeogeography, Palaeoclimatology, Palaeoecology*, v. 244, p. 71–88, doi: 10.1016/j.palaeo.2006.06.024.
- Nomade, S., Knight, K.B., Beutel, E., Renne, P.R., Verati, C., Féraud, G., Marzoli, A., Youbi, N., and Bertrand, H., 2007, Chronology of the Central Atlantic magmatic province: Implications for the Central Atlantic rifting processes and the Triassic-Jurassic biotic crisis: *Palaeogeography, Palaeoclimatology, Palaeoecology*, v. 244, p. 326–344, doi: 10.1016/j.palaeo.2006.06.034.
- O'Dogherty, L., Carter, E.S., Dumitrica, P., Goričan, Š., De Wever, P., Hungerbühler, A., Bandini, A.N., and Takemura, A., 2009a, Catalogue of Mesozoic radiolarian genera. Part 1: Triassic: *Geodiversitas*, v. 31, p. 213–270.
- O'Dogherty, L., Carter, E.S., Dumitrica, P., Goričan, Š., De Wever, P., Bandini, A.N., Baumgartner, P.O., and Matsuoka, A., 2009b, Catalogue of Mesozoic radiolarian genera. Part 2: Jurassic-Cretaceous: *Geodiversitas*, v. 31, p. 271–356.
- Orr, J.C., Fabry, V.J., Aumont, O., Bopp, L., Doney, S.C., Feely, R.A., Gnanadesikan, A., Gruber, N., Ishida, A., Joos, F., Key, R.M., Lindsay, K., Maier-Reimer, E., Matear, R., Monfray, P., Mouchet, A., Najjar, R.G., Plattner, G.K., Rodgers, K.B., Sabine, C.L., Sarmiento, J.L., Schlitzer, R., Slater, R.D., Totterdell, I.J., Weirig, M.F., Yamanaka, Y., and Yool, A., 2005, Anthropogenic ocean acidification over the twenty-first century and its impact on calcifying organisms: *Nature*, v. 437, p. 681–686, doi: 10.1038/nature04095.
- Pálffy, J., Demény, A., Haas, J., Hetényi, M., Orchard, M.J., and Vető, I., 2001, Carbon isotope anomaly and other geochemical changes at the Triassic-Jurassic boundary from a marine section in Hungary: *Geology*, v. 29, p. 1047–1050, doi: 10.1130/0091-7613(2001)029<1047:CIAAOG>2.0.CO;2.
- Pálffy, J., Demény, A., Haas, J., Carter, E.S., Görög, A., Halász, D., Oravecz-Scheffer, A., Hetényi, M., Márton, E., Orchard, M.J., Ozsvárt, P., Vető, I., and Zajzon, N., 2007, Triassic-Jurassic boundary events inferred from integrated stratigraphy of the Csóvár section, Hungary: *Palaeogeography, Palaeoclimatology, Palaeoecology*, v. 244, p. 11–33, doi: 10.1016/j.palaeo.2006.06.021.
- Ruhl, M., Kürschner, W.M., and Krystyn, L., 2009, Triassic-Jurassic organic carbon isotope stratigraphy of key sections in the western Tethys realm (Austria): *Earth and Planetary Science Letters*, v. 281, p. 169–187, doi: 10.1016/j.epsl.2009.02.020.
- Schaltegger, U., Guex, J., Bartolini, A., Schoene, B., and Ovtcharova, M., 2008, Precise U-Pb age constraints for end-Triassic mass extinction, its correlation to volcanism and Hettangian post-extinction recovery: *Earth and Planetary Science Letters*, v. 267, p. 266–275, doi: 10.1016/j.epsl.2007.11.031.
- Schlager, W., 2003, Benthic carbonate factories of the Phanerozoic: *International Journal of Earth Sciences*, v. 92, p. 445–464, doi: 10.1007/s00531-003-0327-x.
- Sepkoski, J.J., Jr., 1996, Patterns of the Phanerozoic extinction: A perspective from global data bases, in Walliser, O.H., eds., *Global Events and Event Stratigraphy in the Phanerozoic*: Berlin, Springer Verlag, p. 53–80.
- Stampfli, G.M., and Hochard, C., 2009, Plate tectonics of the Alpine realm, in Murphy, J.B., Keppie, J.D., and Hynes, A.J., eds., *Ancient Orogens and Modern Examples*: Geological Society of London Special Publication 327, p. 89–111.
- Tanner, L.H., Lucas, S.G., and Chapman, M.G., 2004, Assessing the record and causes of Late Triassic extinctions: *Earth-Science Reviews*, v. 65, p. 103–139, doi: 10.1016/S0012-8252(03)00082-5.
- Tekin, U.K., 2002, Lower Jurassic (Hettangian-Sinemurian) radiolarians from the Antalya Nappes, Central Taurids, southern Turkey: *Micropaleontology*, v. 48, p. 177–205, doi: 10.2113/48.2.177.
- Tomašových, A., and Siblík, M., 2007, Evaluating compositional turnover of brachiopod communities during end-Triassic mass extinction (northern calcareous Alps): Removal of dominant groups, recovery and community reassembly: *Palaeogeography, Palaeoclimatology, Palaeoecology*, v. 244, p. 170–200, doi: 10.1016/j.palaeo.2006.06.028.
- Van de Schootbrugge, B., Tremolada, F., Rosenthal, Y., Bailey, T.R., Feist-Burkhardt, S., Brinkhuis, H., Pross, J., Kent, D.V., and Falkowski, P.G., 2007, End-Triassic calcification crisis and blooms of organic-walled 'disaster species': *Palaeogeography, Palaeoclimatology, Palaeoecology*, v. 244, p. 126–141, doi: 10.1016/j.palaeo.2006.06.026.
- Van de Schootbrugge, B., Payne, J.L., Tomašových, A., Pross, J., Fiebig, J., Benbrahim, M., Follmi, K.B., and Quan, T.M., 2008, Carbon cycle perturbation and stabilization in the wake of the Triassic-Jurassic boundary mass-extinction event: *Geochemistry, Geophysics, Geosystems*, v. 9, p. Q04028, doi: 10.1029/2007GC001914.
- Van de Schootbrugge, B., Quan, T.M., Lindstrom, S., Puttmann, W., Heunisch, C., Pross, J., Fiebig, J., Petschik, R., Rohling, H.G., Richo, S., Rosenthal, Y., and Falkowski, P.G., 2009, Floral changes across the Triassic/Jurassic boundary linked to flood basalt volcanism: *Nature Geoscience*, v. 2, p. 589–594.
- Vlahović, I., Tišljár, J., Velić, I., and Matičec, D., 2005, Evolution of the Adriatic carbonate platform: *Palaeogeography, Palaeoclimatology, Palaeoecology*, v. 220, p. 333–360, doi: 10.1016/j.palaeo.2005.01.011.
- Von Hillebrandt, A., Krystyn, L., and Kuerschner, W.M., 2007, A candidate GSSP for the base of the Jurassic in the northern calcareous Alps (Kuhjoch section, Karwendel Mountains, Tyrol, Austria): *International Sub-commission on Jurassic Stratigraphy Newsletter*, v. 34, p. 2–20.
- Ward, P.D., Garrison, G.H., Williford, K.H., Kring, D.A., Goddwin, D., Beattie, M.J., and McRoberts, C.A., 2007, The organic carbon isotopic and paleontological record across the Triassic-Jurassic boundary at the candidate GSSP section at Ferguson Hill, Muller Canyon, Nevada, USA: *Palaeogeography, Palaeoclimatology, Palaeoecology*, v. 244, p. 281–289, doi: 10.1016/j.palaeo.2006.06.042.
- Williford, K.H., Ward, P.D., Garrison, G.H., and Buick, R., 2007, An extended organic carbon-isotope record across the Triassic-Jurassic boundary in the Queen Charlotte Islands, British Columbia, Canada: *Palaeogeography, Palaeoclimatology, Palaeoecology*, v. 244, p. 290–296, doi: 10.1016/j.palaeo.2006.06.032.
- Wissler, L., Funk, H., and Weissert, H., 2003, Response of Early Cretaceous carbonate platforms to changes in atmospheric carbon dioxide levels: *Palaeogeography, Palaeoclimatology, Palaeoecology*, v. 200, p. 187–205, doi: 10.1016/S0031-0182(03)00450-4.
- Zachos, J.C., Röhl, U., Schellenberg, S., Sluijs, A., Hodell, D.A., Kelly, D.C., Thomas, E., Nicolo, M., Raffi, I., Jourens, L.J., McCarren, H., and Kroon, D., 2005, Rapid acidification of the ocean during the Paleocene-Eocene thermal maximum: *Science*, v. 308, p. 1611–1615, doi: 10.1126/science.1109004.

MANUSCRIPT RECEIVED 24 AUGUST 2009
 REVISED MANUSCRIPT RECEIVED 25 NOVEMBER 2009
 MANUSCRIPT ACCEPTED 30 NOVEMBER 2009

Printed in the USA